MISSOURI
S&T

Missouri University of Science and Technology

Scholars' Mine

Chemistry Faculty Research & Creative Works   Chemistry

01 Sep 1988

Transport Properties of Ground State Oxygen Atoms

Paul M. Holland

Louis Biolsi Jr.
Missouri University of Science and Technology, biolsi@mst.edu

Follow this and additional works at: https://scholarsmine.mst.edu/chem_facwork

Part of the Chemistry Commons

Recommended Citation

Transport properties of ground state oxygen atoms

Paul M. Holland

General Research Corporation, P. O. Box 6770, Santa Barbara, California 93160-6770

Louis Biolsi

Department of Chemistry, University of Missouri-Rolla, Rolla, Missouri 65401

The transport properties of dilute monatomic gases depend on the two body interactions between like atoms. When two ground state oxygen atoms interact, they can follow any of 18 potential energy curves corresponding to O_2, all of which contribute to the transport properties of the ground state atoms. Transport collision integrals have been calculated for those interactions with an attractive minimum in the potential by accurately representing *ab initio* quantum mechanical potential energy curves with the Hulburt–Hirschfelder potential. Repulsive *ab initio* potential energy curves have been accurately represented either with the exponential repulsive potential or with an exponential repulsive potential with an additional Gaussian term to model a shoulder-like feature on the repulsive wall. Results are given for viscosity, thermal conductivity, and diffusion and they are compared with previous theoretical calculations.

I. INTRODUCTION

Knowledge of the thermophysical properties of oxygen atoms is important in the chemistry and physics of the upper atmosphere[1] and in a variety of applications involving air at high temperatures.[2,3] Molecular oxygen is 50% dissociated at about 3500 K. Experimental thermophysical property data is sparse[4-6] for atomic oxygen because of the high temperatures required.

Thus it is necessary to use the kinetic theory of gases[7] to obtain the transport properties of oxygen atoms. The transport properties depend on the two body interaction potentials between two oxygen atoms. When two ground state (^3P) oxygen atoms interact they can follow[8] any of 18 potential energy curves corresponding to the O_2 molecule. These states are listed in Table I and are generally classified as having either an attractive potential well or as being repulsive (based on the *ab initio* quantum mechanical calculations of the potential energy curves by Saxon and Liu[9]).

II. THE O–O INTERACTION POTENTIALS

Since the overall transport properties of the ground state oxygen atoms are obtained by averaging the transport properties for each of the 18 molecular states according to their degeneracies,[10] each of the different states must be considered, using the best interaction potential energy curve available. The SCF-CI calculations of the O_2 potential energy curves by Saxon and Liu[9] have been used for our calculations.

The seven states with a significant attractive minimum have been fit with the Hulburt–Hirschfelder (HH) potential.[11,12] This potential has the reduced form

$$V_{HH}^* = e^{-2a(r^*/d - 1)} - 2e^{-a(r^*/d - 1)}$$
$$+ \beta(r^*/d - 1)^3 [1 + \gamma(r^*/d - 1)] e^{-2a(r^*/d - 1)},$$
(1)

where

$$V^* = V/\epsilon, \quad r^* = r/\sigma, \quad d = r_e/\sigma,$$

$$a = \omega_e/(2\sqrt{B_e \epsilon'}), \quad \beta = ca^3, \quad \gamma = ba,$$

$$c = 1 + a_1\sqrt{\epsilon'/a_0}, \quad b = 2 - (7/12 - e'a_2/a_0)/c,$$

$$a_0 = \frac{\omega_e^2}{4B_e}, \quad a_1 = -1 - \frac{\alpha_e \omega_e}{6B_e^2}, \quad a_2 = \frac{5}{4}a_1^2 - \frac{2\omega_e \chi_e}{3B_e}.$$

Also, V is the potential energy, r is the interatomic separation, ϵ is the depth of the potential well, r_e is the interatomic separation corresponding to ϵ, ϵ' is the well depth in wave numbers, ω_e is the fundamental vibrational frequency, $\omega_e \chi_e$ is the anharmonicity constant, B_e is the rotational constant, α_e is the rotation–vibration coupling constant, and σ is the smallest interatomic separation at which the potential is zero (the effective hard sphere diameter). The HH potential reduces to the Morse potential if $c = 0$.

The HH potential is probably the best general purpose

TABLE I. Molecular states for two interacting ground state (^3P) oxygen atoms.

Attractive minima	Repulsive	Repulsive with shoulder
$X\,^3\Sigma_g^-$	$1\,^1\Pi_u$ (*)[a]	$1\,^3\Pi_u$ (*)
$a\,^1\Delta_g$	$2\,^1\Sigma_g^+$	$1\,^3\Pi_g$ (*)
$b\,^1\Sigma_g^+$	$2\,^3\Sigma_u^+$	$1\,^1\Pi_g$ (*)
$c\,^1\Sigma_u^-$	$^5\Sigma_u^-$ (*)	
$C\,^3\Delta_u$	$^5\Pi_u$ (*)	
$A\,^3\Sigma_u^+$	$^5\Delta_g$ (*)	
$^5\Pi_g$	$1\,^5\Sigma_g^+$ (*)	
	$2\,^5\Sigma_g^*$	

[a] The symbol (*) means that these states actually have a small attractive minimum according to the calculations of Saxon and Liu (Ref. 9). Their spectroscopic notation has been used.

potential for fitting atom–atom interactions with an attractive minimum in the potential.[8,13–16] It accurately reproduces "experimental" RKR potentials for most atom–atom and atom–ion interactions[13,14,17,18] and can reproduce the local maxima often found at larger interatomic separations for atom–atom interactions.[19–23] A computer code has recently been developed[24–26] which calculates the transport collision integrals for the HH potential. The computed results for monatomic argon,[27] lithium,[28] and sodium[29] are in very good agreement with the experimental transport properties for these gases.

It should be noted that the HH potential depends only on the spectroscopic constants of the dimer. If these constants are known, then the HH potential can be used without adjustable parameters. This procedure allows thermophysical properties to be computed quite accurately. Alternatively, a, β, and γ in the HH potential can be used[26,28,29] as adjustable parameters for obtaining accurate fits to *ab initio* quantum mechanical potential energy curves. We have used a nonlinear Nelder–Mead simplex optimization procedure[30,31] to simultaneously fit the four HH parameters a, β, γ, and ϵ for various values of the fifth, σ, for the seven states of O_2 with significant attractive minima listed in the first column of Table I. An example of the excellent fits that we obtain is given for the a $^1\Delta_g$ state in Fig. 1. This is typical of the fits for these states. Another example of the fit, for the $^5\Pi_g$ state which has a much smaller attractive minimum, is shown in Fig. 2. In the case of the ground $X\,^3\Sigma_g^-$ state, the Saxon and Liu[9] *ab initio* results were only available for the inner repulsive part of the potential at a single point, which was below 1 eV. In order to ensure a reasonable fit for this part of the potential, some additional higher energy values generated from the spectroscopic HH potential were included in our fitting procedure for this state.

A second group of eight states, listed in the second column of Table I, can be fit using the exponential repulsive
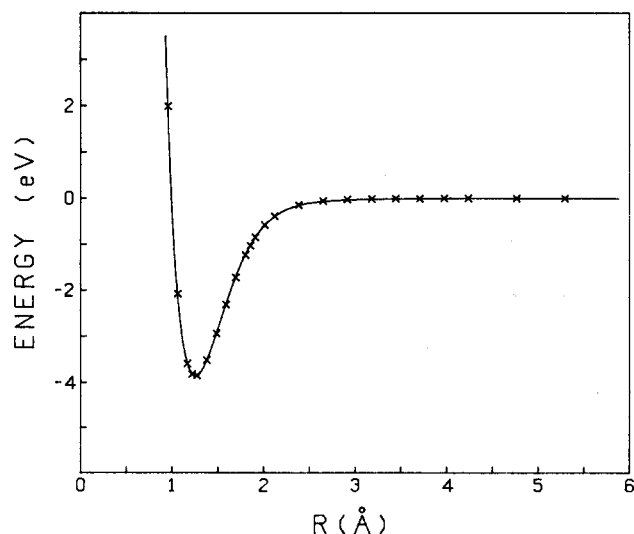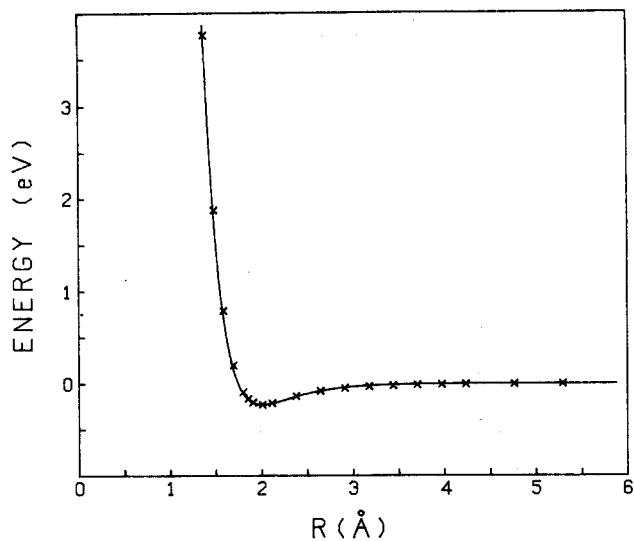

FIG. 2. A comparison of the simplex fit of the HH potential to the SL potential (Ref. 9) for the $^5\Pi_g$ state of O_2. The solid line is the result of the simplex fit and the points (X) are the SL results.

(ER) potential, given by

$$V_R^* = e^{-\gamma(r^* - 1)}, \tag{2}$$

where

$$V^* = V/\epsilon, \quad r^* = r/\sigma.$$

The symbols σ and ϵ are used here as length and energy scaling parameters, in order to provide a properly reduced form of the potential for the computations, and γ is used as an adjustable parameter. For these states, since the level of monatomic oxygen in the atmosphere drops below 1% due to ionization above 20 000 K (and thus is outside the range of interest for these calculations), the fitting procedure for the ER potentials was modified by limiting it to *ab initio*

FIG. 1. A comparison of the simplex fit of the HH potential to the SL potential (Ref. 9) for the a $^1\Delta_g$ state of O_2. The solid line is the result of the simplex fit and the points (X) are the SL results.

FIG. 3. A comparison of the simplex fit of the ER potential to the SL potential (Ref. 9) for the 2 $^1\Sigma_g^+$ state of O_2. The solid line is the result of the simplex fit and the points (X) are the SL results.

FIG. 4. A comparison of the simplex fit of the ER potential to the SL potential (Ref. 9) for the $2\,^5\Sigma_g^+$ state of O_2. The solid line is the result of the simplex fit and the points (X) are the SL results.
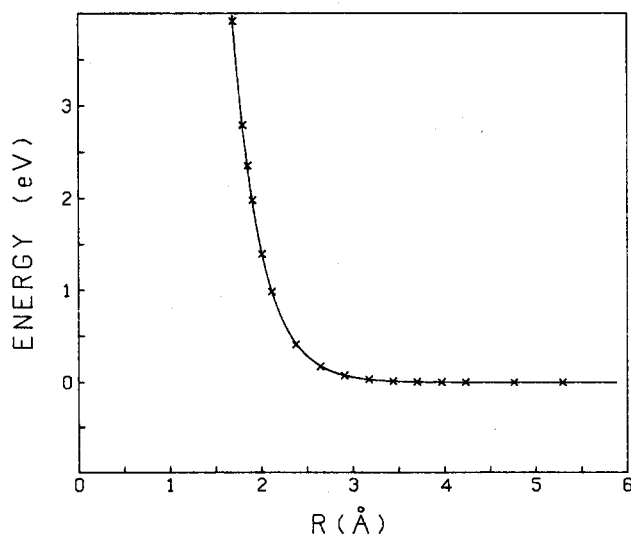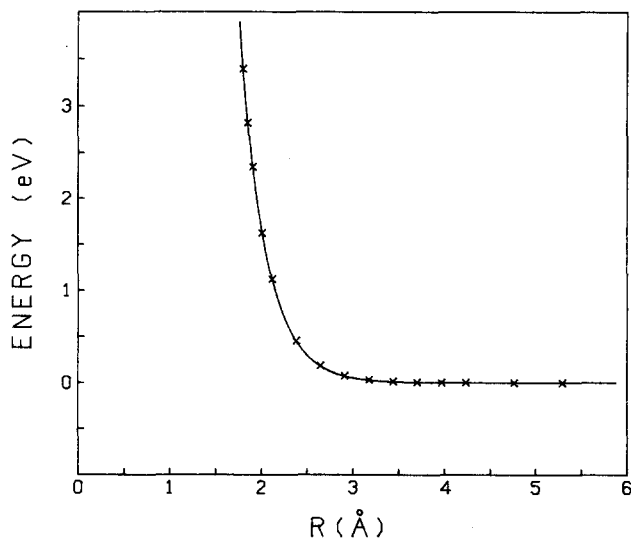

FIG. 6. A comparison of the simplex fit of the ERG potential to the SL potential (Ref. 9) for the $1\,^3\Pi_g$ state of O_2. The solid line is the result of the simplex fit and the points (X) are the SL results.

results below 4.5 eV to improve the quality of the fit in the region of greatest interest. However, in each case, comparisons at higher energies were also made to ensure that the resulting potentials were reasonable well beyond the limits of the fits themselves.

Examples of the fits are given for the relatively low lying $2\,^1\Sigma_g^+$ state and for the higher $2\,^5\Sigma_g^+$ state in Figs. 3 and 4, respectively. The calculations of Saxon and Liu[9] indicate that the $2\,^1\Sigma_g^+$ state has a change in slope (i.e., a "shoulder") above 5 eV (see Fig. 1 of Ref. 9) but Fig. 3 shows an excellent fit to be obtained within the energy range of interest.
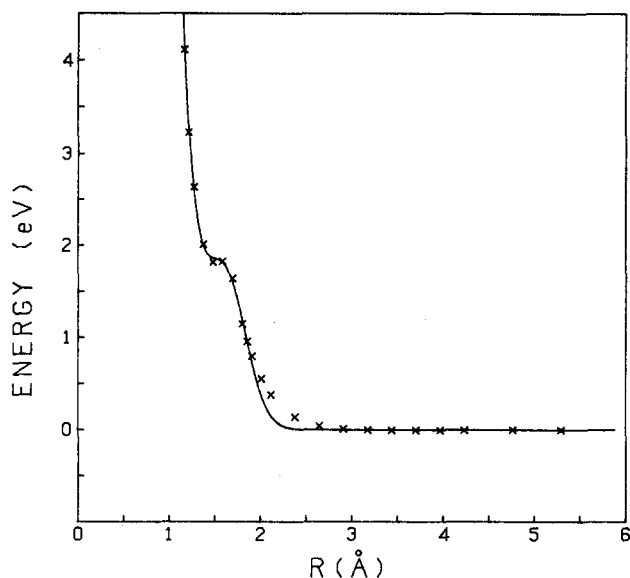
The final group of three states listed in the third column

of Table I have repulsive potential energy curves which exhibit a shoulder-like feature below 5 eV. These have been fit with a modified ER potential (called ERG) which includes an additional Gaussian term to model the shoulder. This potential has the form

$$V_{ERG}^* = K_{ERG}\,(e^{-\gamma(r^* - 1)} + Ae^{-B(r^* - r_s^*)^2}),\qquad (3)$$

where

$$V^* = V/\epsilon \quad r^* = r/\sigma \quad r_s^* = r_s/\sigma$$

$$K_{ERG} = \frac{1}{1 + Ae^{-B(1 - r_s^*)^2}}.$$

FIG. 5. A comparison of the simplex fit of the ERG potential to the SL potential (Ref. 9) for the $1\,^3\Pi_u$ state of O_2. The solid line is the result of the simplex fit and the points (X) are the SL results.
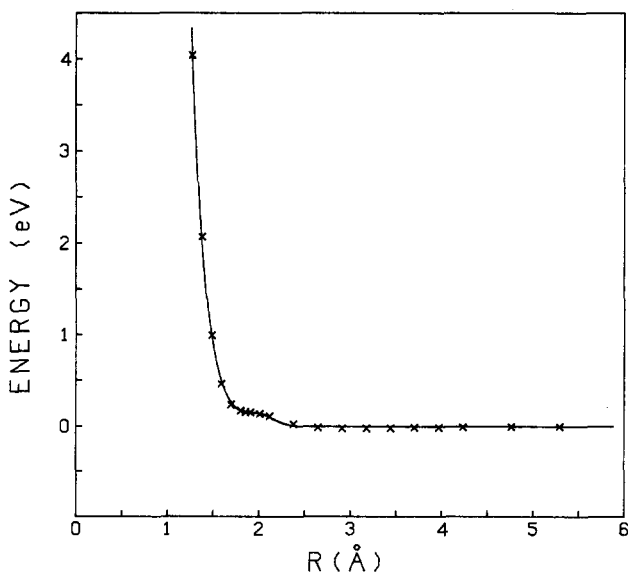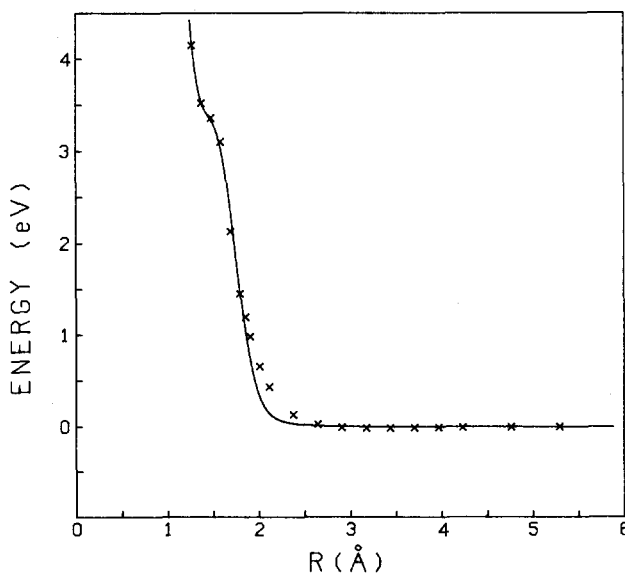

FIG. 7. A comparison of the simplex fit of the ERG potential to the SL potential (Ref. 9) for the $1\,^1\Pi_g$ state of O_2. The solid line is the result of the simplex fit and the points (X) are the SL results.

TABLE II. Spectroscopic constants for the O_2 states with an attractive minimum.[a]

	$X\,^3\Sigma_g^-$	$a\,^1\Delta_g$	$b\,^1\Sigma_g^+$	$c\,^1\Sigma_u^-$	$C\,^3\Delta_u$	$A\,^3\Sigma_u^+$
ϵ(eV)	5.2136	4.2259	3.5685	1.066	0.867	0.8243
ω_e(cm^{-1})	1580.2	1483.5	1432.8	794.2	850	799.07
$\omega_e\chi_e$ (cm^{-1})	11.98	12	14.00	12.73	20	12.16
B_e (cm^{-1})	1.4456	1.4264	1.4004	0.915	0.96	0.9106
α_e(cm^{-1})	0.0159	0.0171	0.0182	0.0139	0.026	0.0141
r_e(Å)	1.2075	1.2156	1.2269	1.517	1.48	1.5215

[a]The spectroscopic constants tabulated above are from Huber and Herzberg (Ref. 34) except that the value of ϵ for the $A\,^3\Sigma_u^+$ state is from Krupenie (Ref. 14).

Again, σ and ϵ represent length and energy scaling parameters for this potential with r_s representing the location of the Gaussian shoulder, and A, B, and γ are used as adjustable parameters. The fits obtained for these three states are

TABLE III. Ratio of the RKR to the spectroscopic HH potential for the ground $X\,^3\Sigma_g^-$ state of O_2 as a function of interatomic separation.

r(Å)	RKR/HH	r(Å)	RKR/HH
0.9761	1.05	1.246	1.00
0.9776	1.05	1.263	1.00
0.9791	1.05	1.288	1.00
0.9807	1.04	1.308	1.00
0.9824	1.04	1.326	1.00
0.9841	1.04	1.342	1.00
0.9858	1.04	1.357	1.00
0.9876	1.03	1.371	1.00
0.9894	1.03	1.385	1.00
0.9913	1.03	1.398	1.00
0.9933	1.03	1.410	1.00
0.9953	1.02	1.423	1.00
0.9974	1.02	1.435	1.00
0.9995	1.02	1.446	1.00
1.002	1.01	1.458	1.00
1.004	1.02	1.469	0.99
1.006	1.02	1.481	0.99
1.009	1.01	1.492	0.99
1.011	1.02	1.503	0.99
1.014	1.01	1.514	0.99
1.016	1.02	1.524	0.99
1.019	1.01	1.535	0.99
1.022	1.01	1.546	0.98
1.025	1.01	1.556	0.98
1.028	1.01	1.567	0.98
1.031	1.01	1.577	0.97
1.035	1.00	1.588	0.97
1.038	1.01	1.598	0.97
1.042	1.00	1.609	0.97
1.045	1.01	1.619	0.96
1.049	1.01	1.630	0.96
1.054	1.00	1.640	0.95
1.058	1.00	1.651	0.95
1.063	1.00	1.661	0.94
1.068	1.00	1.672	0.94
1.073	1.00	1.683	0.94
1.079	1.00	1.693	0.93
1.085	1.00	1.704	0.92
1.091	1.00	1.715	0.92
1.099	1.00	1.725	0.91
1.107	1.00	1.736	0.90
1.116	1.00	1.747	0.89
1.127	1.00	1.758	0.88
1.141	1.00	1.769	0.88
1.159	1.00	1.780	0.87
1.173	1.00	1.792	0.86

shown in Figs. 5–7. Of these, the fit for the 1 $^3\Pi_u$ state was limited to *ab initio* energies below 4.5 eV. The shoulder-like features in these potentials are the result of avoided curve crossings as the figures in Refs. 32 and 33 make clear for the $^3\Pi_g$ and $^1\Pi_g$ states. The quality of the fit at the lowest energies (below 0.5 eV) for the $^3\Pi_g$ and $^1\Pi_g$ states was compromised somewhat in order to obtain an accurate fit in the 1–3 eV region of greatest interest for these calculations.

III. SPECTROSCOPIC POTENTIALS

The spectroscopic constants needed to obtain the HH potential directly from the spectroscopy of the dimers are known for six of the states of O_2 with a minimum in the potential. These are shown in Table II (while the $^5\Pi_g$ state has a very shallow minimum according to the calculations of Saxon and Liu,[9] spectroscopic constants have not been determined for this state).

Comparisons of the spectroscopically determined HH potential with the available RKR potentials[14] for two of these states are shown in Tables III and IV. In addition, the

TABLE IV. Ratio of the RKR to the spectroscopically determined HH potential energy for the $A\,^3\Sigma_u^+$ excited state of O_2 as a function of interatomic separation.

| r(Å)	RKR/HH	r(Å)	RKR/HH
1.297	− 0.91	1.600	1.00
1.298	− 2.37	1.638	1.00
1.301	4.26	1.668	1.00
1.304	1.85	1.696	1.00
1.306	1.66	1.722	1.00
1.310	1.30	1.748	1.00
1.313	1.24	1.772	1.00
1.317	1.16	1.797	1.00
1.322	1.08	1.822	1.01
1.326	1.08	1.846	1.00
1.332	1.03	1.872	1.01
1.337	1.03	1.897	1.01
1.343	1.03	1.925	1.01
1.350	1.01	1.953	1.01
1.357	1.01	1.982	1.01
1.366	1.00	2.014	1.01
1.375	1.00	2.050	1.02
1.385	1.00	2.089	1.04
1.397	1.00	2.131	1.05
1.411	1.00	2.182	1.10
1.429	1.00	2.245	1.20
1.454	1.00	2.323	1.40
		2.423	1.76
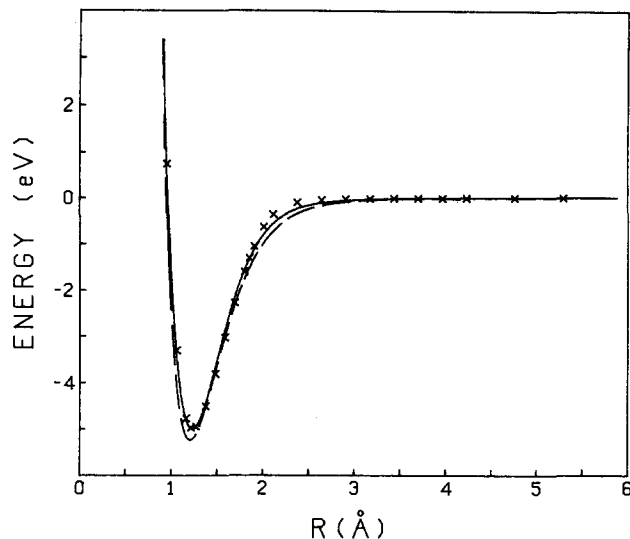
FIG. 8. A comparison of the simplex fit of the HH potential to the SL potential (Ref. 9) with the spectroscopically determined HH potential for the ground $X\,^3\Sigma_g^-$ state of O_2. The solid line is the result of the simplex fit, the dashed line is obtained using the experimental spectroscopic constants, and the points (X) are the SL results.

ratio of the RKR to the HH potential is 1.00 for all values of r for the $a\,^1\Delta_g$ and $b\,^1\Sigma_g^+$ states. Thus agreement is seen to be excellent for each of the states except for the $A\,^3\Sigma_u^+$ state at small r (where the HH potential has a steeper repulsive wall than the RKR potential) and at large r (where the HH potential goes to zero faster than the RKR potential). The spectroscopic constants listed in Table II are from Huber and Herzberg[34] except that ϵ for the $A\,^3\Sigma_u^+$ state is from Krupenie.[14] The Huber and Herzberg value of ϵ for this state gives an HH potential which has much poorer agreement with the RKR potential than that shown in Table IV.

Comparisons of the spectroscopically determined HH potentials with our fits using the ab initio results of Saxon and Liu[9] for the ground $X\,^3\Sigma_g^-$ and $A\,^3\Sigma_g^+$ states are shown in Figs. 8 and 9, respectively. The potentials are generally seen to agree quite well except for differences in ϵ. In the case of the ground $X\,^3\Sigma_g^-$ state, it should be noted that some additional values from the spectroscopic HH potential were used in fitting the inner repulsive wall of the potential.

IV. TRANSPORT PROPERTIES OF ATOMIC OXYGEN

According to the kinetic theory of gases,[7] the viscosity of a pure gas η is given by

$$\eta = \frac{5}{16}\left(\frac{mkT}{\pi}\right)^{1/2}\frac{1}{\sigma^2\Omega^{(2,2)*}}, \tag{4}$$

where m is the mass, k is Boltzmann's constant, T is the temperature, and $\sigma^2\Omega^{(2,2)*}$ is the viscosity collision integral. Also, the translational thermal conductivity of a pure gas λ, is given by

$$\lambda = \frac{25}{32}\left(\frac{kT}{\pi m}\right)^{1/2}\frac{c_v}{\sigma^2\Omega^{(2,2)*}}, \tag{5}$$

where c_v is the specific heat per atom, taken to be $3k/2$, and the self-diffusion coefficient D is given by

$$D = \frac{3}{8}\left(\frac{kT}{\pi m}\right)^{1/2}\frac{1}{\rho\sigma^2\Omega^{(1,1)*}}, \tag{6}$$

where ρ is the particle density and $\sigma^2\Omega^{(1,1)*}$ is the diffusion collision integral.

Using the transport collision integral program developed previously,[24,26] diffusion and viscosity collision integrals have been calculated for each of the 18 molecular states of O_2 that dissociate to ground state oxygen atoms, using our potential fits to the ab initio potential energy curves of Saxon
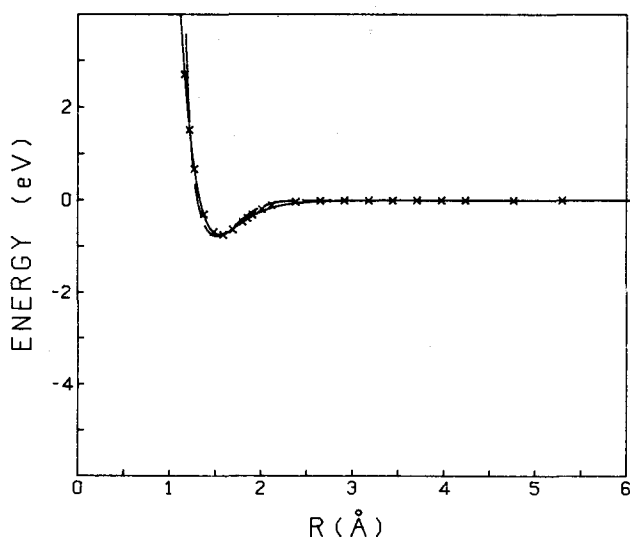

FIG. 9. A comparison of the simplex fit of the HH potential to the SL potential (Ref. 9) with the spectroscopically determined HH potential for the $A\,^3\Sigma_u^+$ state of O_2. The solid line is the result of the simplex fit, the dashed line is obtained using the experimental spectroscopic constants, and the points (X) are the SL results.

TABLE V. The diffusion collision integral $\sigma^2\Omega^{(1,1)*}$ and the viscosity collision integral $\sigma^2\Omega^{(2,2)*}$ for the ground (^3P) state of oxygen atoms as a function of temperature.

$T(\mathrm{K})$	$\sigma^2\Omega^{(1,1)*}$ (Å²)	$\sigma^2\Omega^{(2,2)*}$ (Å²)
2 000	4.9761	5.6880
2 500	4.6787	5.3606
3 000	4.4452	5.1060
3 500	4.2534	4.8989
4 000	4.0922	4.7255
4 500	3.9531	4.5755
5 000	3.8305	4.4447
6 000	3.6238	4.2238
7 000	3.4539	4.0430
8 000	3.3103	3.8906
9 000	3.1865	3.7589
10 000	3.0783	3.6433
11 000	2.9819	3.5404
12 000	2.8954	3.4475
13 000	2.8171	3.3630
14 000	2.7455	3.2857
15 000	2.6801	3.2143
16 000	2.6201	3.1480
17 000	2.5643	3.0864
18 000	2.5124	3.0286
19 000	2.4639	2.9748
20 000	2.4186	2.9239

TABLE VI. The theoretically calculated transport properties viscosity η, thermal conductivity λ, and self-diffusion D, for ground state oxygen atoms as a function of temperature at 1 atm.

T(K)	$\eta(10^{-4}$ kg/m s)	λ(W/m K)	$D(10^{-3}$ m^2/s)
2 000	0.8395	0.1636	1.181
2 500	0.9963	0.1941	1.756
3 000	1.145	0.2232	2.429
3 500	1.290	0.2513	3.199
4 000	1.429	0.2785	4.062
4 500	1.565	0.3051	5.018
5 000	1.699	0.3310	6.064
6 000	1.958	0.3816	8.448
7 000	2.209	0.4305	11.16
8 000	2.454	0.4783	14.23
9 000	2.694	0.5251	17.64
10 000	2.930	0.5710	21.38
11 000	3.163	0.6163	25.45
12 000	3.393	0.6611	29.87
13 000	3.620	0.7054	34.60
14 000	3.845	0.7493	39.68
15 000	4.069	0.7928	45.07
16 000	4.290	0.8360	50.78
17 000	4.510	0.8789	56.82
18 000	4.730	0.9217	63.19
19 000	4.947	0.9641	69.87
20 000	5.164	1.007	76.87

TABLE VII. Ratios of the viscosity collision integrals $\sigma^2\Omega^{(2,2)*}$ obtained for ground state oxygen atoms by Yun and Mason (Ref. 35) and by Capitelli and Ficocelli (Ref. 40) to the results obtained in this work.

T(K)	(Ref. 35)/(this work)	(Ref. 40)/(this work)
2 000	1.08	0.96
2 500	1.09	
3 000	1.09	
3 500	1.09	
4 000	1.09	0.99
4 500	1.10	
5 000	1.10	
6 000	1.10	1.00
7 000	1.10	
8 000	1.10	1.00
9 000	1.10	
10 000	1.10	1.01
11 000	1.10	
12 000	1.10	1.01
13 000	1.10	
14 000	1.10	1.02
15 000	1.10	
16 000		1.02
18 000		1.02
20 000		1.03

curves of Saxon and Liu.[9] The individual collision integrals were then degeneracy averaged.[10] The resulting collision integrals are given in Table V and the transport properties are given in Table VI.

V. DISCUSSION

The first rigorous calculation of the transport collision integrals of ground state oxygen atoms were reported by Yun and Mason[35] (YM). These calculations were based on the representation of the 18 O_2 potential energy curves obtained by Vanderslice et al.[8,18] In general, they used the spectroscopically determined RKR potential for the bound states and fitted the RKR results with either the inverse power attractive potential or the exponential-six potential and then used the tabulated transport collision integrals for these potentials.[36,37] The potential energy curves for the repulsive states were estimated by using a qualitative semiempirical quantum mechanical technique based on the perfect pairing method.[8,38] These results were then fitted with the ER potential for which the transport collision integrals are tabulated.[39] A comparison of the degeneracy averaged viscosity collision integrals obtained by YM with our results is shown in the second column of Table VII. Agreement is reasonably good (approximately a 10% difference at all temperatures considered) despite the fact that the potentials used by YM are generally quite different than those used in our work. This suggests that the variety of approximations used by YM were well chosen.

Capitelli and Ficocelli[40] (CF) calculated the transport collision integrals of ground state oxygen atoms by fitting the *ab initio* quantum mechanical potential energy curves obtained by Schaefer and Harris[41] with the ER potential for repulsive states and with the Morse potential for states with

an attractive minimum. They then used the tabulated transport collision integrals for these potentials.[39,42] A comparison of their degeneracy averaged viscosity collision integrals with our results is shown in the third column of Table VII. There is only a difference of a few percent over the temperature range considered.

Saxon and Liu[9] (SL) compared the spectroscopic constants obtained from their calculations for the bound states with those obtained by Schaefer and Harris[41] (SH). The more recent SL results agree better with the experimental spectroscopic constants than do the SH results for each of the calculated constants. This is especially important for ϵ since the well depth has an important effect on the transport collision integrals. Compared with experimental values for ϵ, the average error in the SL calculations for six states is 6.1% while the average error in the SH calculation is 27%. Saxon and Liu[9] also concluded that their calculations for repulsive states should be a substantial improvement over the earlier minimum basis set SH calculations. Thus, we would expect collision integral calculations based on the SL potential energy curves to be more accurate than calculations based on the SH potential energy curves.

That the HH potential is perhaps the best general purpose atom–atom potential is supported by the results in Tables III and IV which show the HH potential to mimic the experimental RKR potential very accurately in most cases. To provide a further test, we have also calculated the transport collision integrals using experimental (spectroscopic) HH parameters for the six states of O_2 listed in Table II. We find there to be less than a 3% difference from 2000 to 20 000 K between the viscosity collision integrals obtained using the *ab initio* calculations of Saxon and Liu[9] for all states and the viscosity collision integrals obtained when the HH potential is used for the six bound states.

However, the good agreement between the overall re-

TABLE VIII. Ratios of the viscosity collision integrals $\sigma^2\Omega^{(2,2)*}$ calculated theoretically at 10 000 K.

State	YM/SL	CF/SL	HH/SL
$X\,^3\Sigma_g^-$	1.06	1.05	1.10
$a\,^1\Delta_g$	1.02	1.02	1.09
$b\,^1\Sigma_g^+$	0.99	1.01	1.04
$c\,^1\Sigma_u^-$	0.85	0.94	0.92
$C\,^3\Delta_u$	1.03	0.98	0.98
$A\,^3\Sigma_u^+$	1.06	0.99	0.99
rmsd-a[a]	8%	4%	7%
$2\,^1\Sigma_g^+$	0.91	0.97	
$2\,^3\Sigma_u^+$	0.85	0.97	
$1\,^5\Sigma_g^+$	1.09	0.95	
$^5\Sigma_u^-$	1.20	1.09	
$2\,^5\Sigma_g^+$	1.00	0.92	
$1\,^1\Pi_g$	0.97	1.02	
$1\,^1\Pi_u$	0.87	1.09	
$1\,^3\Pi_g$	1.08	1.10	
$1\,^3\Pi_u$	1.23	1.42	
$^5\Pi_g$	1.28	1.06	
$^5\Pi_u$	1.27	0.96	
$^5\Delta_g$	1.10	0.95	
rmsd-r	17%	14%	
rmsd-t	14%	12%	

[a] The symbol rmsd means the root mean square percent difference in the two results being compared; the symbols a, r, and t mean the attractive (bound) states, the repulsive states, and all 18 (total) states, respectively.

sults obtained by us using only the *ab initio* SL potentials and the YM and CF results, and between our *ab initio* results and our results obtained using the HH potential for the bound states masks some differences for individual states. This is shown in Table VIII at 10 000 K, a temperature at which almost all of the oxygen in air exists as oxygen atoms. It can be seen that, at 10 000 K, there are some substantial differences in the viscosity collision integrals for individual states as obtained from the four calculations. The CF collision integrals differ from ours by 10% or less for the various states except for the $1\,^3\Pi_u$ state. If that state were ignored, the CF viscosity collision integrals for the repulsive states would have a root mean square difference from ours of only 6%.

Also notice (column four of Table VIII) that the state-by-state comparison of the viscosity collision integrals based on the HH potential (which Tables III and IV indicate is essentially the experimental RKR potential) with our results based on the *ab initio* SL potentials shows that three of the HH states are "high" and three are "low", leading to the excellent average agreement for all six states.

Unfortunately, there is very limited experimental data relating to the transport properties of oxygen atoms at high temperatures[4–6] and what data is available is for mixtures of oxygen atoms and molecules. Thus direct comparison of our calculations with experimental results is not possible at the present time.

The SCF-CI calculations of the O_2 potential energy curves by Saxon and Liu,[9] on which our calculations are based, should be considerably improved over the minimum basis set potential energy curves of Schaefer and Harris,[41] on which the CF[40] calculations are based. This is discussed in detail by Saxon and Liu.[9] We previously estimated[29] that the thermophysical property calculations for monatomic sodium using theoretical Na_2 potentials were in error by about 10% or less. This estimate was supported by comparison with the limited experimental transport data. We expect the O_2 potential energy curves to be about as accurate as the Na_2 potential energy curves and, on this basis, we estimate the error in the transport properties given in Table VI to be 10%–15% or less.

Finally, the calculations of Moss and Goddard[43] for the $A\,^3\Sigma_u^+$ state of O_2 indicate this state to have a maximum in the potential energy curve while the SL calculations do not indicate this. Our HH spectroscopic parameter calculations indicate this to be a type 3 potential[25]; i.e., it has a maximum but the maximum occurs at slightly negative energies. Only a small change in the values of the spectroscopic parameters would convert this to a type 4 HH potential[25]; i.e., a potential with a maximum at slightly positive energies such as that obtained by Moss and Goddard.[43] Since all of our previous experience with the HH potential has indicated that this potential form is remarkably well suited for reproducing much of the detail of "true" potentials, we would suggest that the $A\,^3\Sigma_u^+$ state probably does have a local maximum. We have used the SL *ab initio* results in the present work rather than those of Moss and Goddard[43] because the results of SL have slightly better values of ϵ which is very important for the calculation of the transport collision integrals.

ACKNOWLEDGMENTS

[1] J. M. Wallace and P. V. Hobbs, *Atmospheric Science* (Academic, New York, 1977).
[2] R. M. Davies and H. E. Toth, in *Proceedings of the Fourth Symposium on Thermophysical Properties*, edited by J. R. Moszynski (ASME, New York, 1968), p. 350.
[3] C. D. Scott, in Prog. Astronaut. Aeronaut. **82**, 273 (1982).
[4] S. Krongelb and M. W. P. Strandberg, J. Chem. Phys. **31**, 1196 (1959).
[5] R. E. Walker, J. Chem. Phys. **34**, 2196 (1961).
[6] R. A. Hartunian and P. V. Marrone, Phys. Fluids **4**, 535 (1961).
[7] J. O. Hirschfelder, C. F. Curtiss, and R. B. Bird, *Molecular Theory of Gases and Liquids* (Wiley, New York, 1954), Chaps. 7 and 8.
[8] J. T. Vanderslice, E. A. Mason, and W. G. Maisch, J. Chem. Phys. **32**, 515 (1960).
[9] R. P. Saxon and B. Liu, J. Chem. Phys. **67**, 5432 (1977).
[10] J. T. Vanderslice, S. Weissman, E. A. Mason, and R. J. Fallon, Phys. Fluids **5**, 155 (1962).
[11] H. M. Hulburt and J. O. Hirschfelder, J. Chem. Phys. **9**, 61 (1941).
[12] H. M. Hulburt and J. O. Hirschfelder, J. Chem. Phys. **35**, 1901 (1961).
[13] D. Steele, E. R. Lippincott, and J. T. Vanderslice, Rev. Mod. Phys. **34**, 239 (1962).
[14] P. H. Krupenie, J. Phys. Chem. Ref. Data **1**, 423 (1972).
[15] G. C. Lie and E. Clementi, J. Chem. Phys. **60**, 1288 (1974).
[16] G. Das and A. C. Wahl, J. Chem. Phys. **44**, 87 (1966).
[17] A. Lofthus and P. H. Krupenie, J. Phys. Chem. Ref. Data **6**, 113 (1977).
[18] J. T. Vanderslice, E. A. Mason, W. G. Maisch, and E. R. Lippincott, J. Chem. Phys. **33**, 614 (1960).
[19] L. Biolsi, J. C. Rainwater, and P. M. Holland, J. Chem. Phys. **77**, 448 (1982).
[20] G. Herzberg, *Molecular Spectra and Molecular Structure. I. Spectra of Diatomic Molecules*, 2nd ed. (Van Nostrand, New York, 1950), p. 425.
[21] R. S. Mulliken, J. Phys. Chem. **41**, 5 (1937).
[22] J. C. Brown and F. A. Matsen, Adv. Chem. Phys. **23**, 161 (1973).

[23]P. F. Fougere and R. K. Nesbet, J. Chem. Phys. **44**, 285 (1966).

[24]J. C. Rainwater, P. M. Holland, and L. Biolsi, Prog. Astronaut. Aeronaut. **82**, 3 (1982).

[25]J. C. Rainwater, P. M. Holland, and L. Biolsi, J. Chem. Phys. **77**, 434 (1982).

[26]J. C. Rainwater, L. Biolsi, K. J. Biolsi, and P. M. Holland, J. Chem. Phys. **79**, 1462 (1983).

[27]P. M. Holland, L. Biolsi, and J. C. Rainwater, Chem. Phys. **98**, 383 (1985).

[28]P. M. Holland, L. Biolsi, and J. C. Rainwater, J. Chem. Phys. **85**, 4011 (1986).

[29]P. M. Holland and L. Biolsi, J. Chem. Phys. **87**, 1261 (1987).

[30]J. A. Nelder and R. Mead, Comput. J. **7**, 308 (1965).

[31]M. S. Caceci and W. P. Catheris, Byte **9**, 340 (1984).

[32]R. P. Saxon and B. Liu, J. Chem. Phys. **73**, 870 (1980).

[33]R. P. Saxon and B. Liu, J. Chem. Phys. **73**, 876 (1980).

[34]K. P. Huber and G. Herzberg, *Molecular Spectra and Molecular Structure. IV. Constants of Diatomic Molecules* (Van Nostrand, New York, 1979), pp. 496–498.

[35]K. S. Yun and E. A. Mason, Phys. Fluids **5**, 380 (1962).

[36]T. Kihara, M. H. Taylor, and J. O. Hirschfelder, Phys. Fluids **3**, 715 (1960).

[37]E. A. Mason, J. Chem. Phys. **22**, 169 (1954).

[38]C. A. Coulson, *Valence* (Oxford University, New York, 1952).

[39]L. Monchick, Phys. Fluids **2**, 695 (1959).

[40]M. Capitelli and E. Ficocelli V, J. Phys. B **5**, 2066 (1972).

[41]H. F. Schaefer and F. E. Harris, J. Chem. Phys. **48**, 4946 (1968).

[42]F. J. Smith and R. J. Munn, J. Chem. Phys. **41**, 3560 (1964).

[43]B. J. Moss and W. A. Goddard III, J. Chem. Phys. **63**, 3523 (1975).